Nonlinearity of Superconducting Transmission Line and Microstrip Resonsator

Orest G. Vendik, *Member, IEEE,* Irina B. Vendik, *Member, IEEE,* and Tatyana B. Samoilova

***Abstract*— The simplest model of nonlinear response of a superconducting thin film is used for modeling the nonlinear phenomena in a superconducting transmission line and a microstrip resonator. The specified characteristic power of the transmission line is suggested to use as a fitting parameter for numerical description of the microstrip line nonlinearity at microwaves. Quantitative agreement of simulated and experimental data has been obtained for the incident power dependent transmission coefficient of a microstrip line section and a high quality microstrip resonator. Numerical results have also been obtained for the power of the third harmonic radiated from the nonlinear resonator.**

***Index Terms*— High-temperature superconductors, nonlinearities, superconducting resonator, superconducting transmission line.**

I. Introduction

WITHIN the last few years interest in the nonlinearity of superconducting films has been renewed. This is basically associated with microwave applications of high-T_c superconductors (HTS's) at microwaves. In the 1970's a nonlinear response of a superconductor to microwave radiation was studied in connection with a design of high quality resonance systems [1], [2]. The interest in applications of microwave components and devices based on HTS films initiated a new wave of investigations of physical phenomena in the superconducting films. In many cases, nonlinear effects limit high-power handling of the HTS films in linear microwave devices and therefore are desired to be suppressed. However, the nonlinear phenomena can be considered as useful effects in the design of microwave signal limiters [3] or frequency mixers [4]. The contribution of the following superconductor nonlinearity mechanisms should be mentioned:

1) nonlinear impedance of weak links between granulars or twin domains in a polycrystalline superconductor [5], [6];
2) current dependence of superconducting charge carrier density in accordance with Ginzburg–Landau equations [7];
3) excitation and movement of Abrikosov vortices [8].

Manuscript received August 2, 1995; revised October 18, 1996. This work was supported by the Science Council on High Temperature Superconductivity under Project 93223. The work of O. G. Vendik was supported by the International Soros Science Education Program under Grant 1048-p.

O. G. Vendik and T. B. Samoilova are with the Electronics Department, Electrotechnical University, St. Petersburg, 197376 Russia.

I. B. Vendik is with the Radio Engineering Department, Electrotechnical University, St. Petersburg, 197376 Russia.

Publisher Item Identifier S 0018-9480(97)00820-X.

It is a well-known fact that under the influence of alternating current the loss in a superconducting transmission line is increased [6]–[11]. One may use the expansion in a power series

$$R_1(t) = \sum_{n=0}^{N} a_n [I(t)]^{2n} \tag{1}$$

where N is a total number of terms of the series expansion which are necessary for an adequate description of the phenomenon. In expansion (1) only even powers are used because the response of a superconductor to the current does not depend on direction of the current. We shall consider the case when the surface resistance of the superconducting film can follow the instantaneous values of the alternating current. It is correct if the relaxation time of the superconducting state in the film is less than the period of the microwave oscillations. The relaxation time of HTS's at liquid nitrogen temperature is less than 10^{-11} s [12]; hence, up to frequency 100 GHz our estimations will be correct. The nonlinearity characterized by the increased resistance which follows the instantaneous values of the current can be called the fast (inertialess) resistive nonlinearity. The inertialessness of the nonlinearity shows up in the generation of higher harmonics of a signal. It is undoubtedly useful to discuss how different mechanisms of nonlinearity mentioned above are exhibited in the numerical values of the coefficients of the series (1). At the same time, the phenomenological description of the superconducting film nonlinearity can be used as well. It will be shown that the phenomenological description of the superconducting film nonlinearity provides numerical results which are in good agreement with experimental data.

II. Nonlinear Dissipation in a Superconducting Transmission Line

A. Model of Nonlinearity

For a phenomenological description of the resistive nonlinearity of a superconducting transmission line, the two first terms of the series (1) will be used. In this case, the resistance per unit length of the line as a function of the microwave current $I(x,t)$ can be presented as follows:

$$R_1(x,t) = R_1 \cdot \left[1 + \frac{I^2(x,t)}{I_0^2}\right]. \tag{2}$$

Here, R_1 is the resistance per unit length of the line in a linear approach, I_0 and is a phenomenological parameter which describes the nonlinear properties of the line. There is no direct connection between I_0 and I_C which determines the appearance of $R_{dc} > 0$. The parameter I_0 should be found experimentally through measurements of the propagation characteristics of the line exposed to the microwave power. One should not rule out a possibility to find I_0 theoretically by consideration of the superconducting film response to a high microwave current. In doing so the current distribution across the film should be taken into account.

B. Nonlinear Dissipation of a Traveling Wave

Inserting (2) into the telegrapher equations for the transmission line one obtains

$$\frac{\partial I(x,t)}{\partial x} = -C_1 \cdot \frac{\partial U(x,t)}{\partial t}$$
$$\frac{\partial U(x,t)}{\partial x} = -\left\{R_1 \cdot \left[1 + \frac{I^2(x,t)}{I_0^2}\right] \cdot I(x,t) + L_1 \cdot \frac{\partial I(x,t)}{\partial t}\right\} \quad (3)$$

where L_1, C_1 are the inductance and the capacitance per unit length of the line, respectively. The equations can be transformed as follows:

$$\frac{\partial^2 I(x,t)}{\partial x^2} = C_1 R_1 \cdot \left[1 + 3 \cdot \frac{I^2(x,t)}{I_0^2}\right] \cdot \frac{\partial I(x,t)}{\partial t} + L_1 C_1 \cdot \frac{\partial^2 I(x,t)}{\partial t^2}. \quad (4)$$

Let us take into consideration the microwave current in the following form:

$$I(x,t) = I_m(x) \cos(\omega t - \beta x). \quad (5)$$

Substitution of (5) into (4) gives for the first harmonic of the microwave signal:

$$\left[\frac{\partial^2 I_m(x)}{\partial x^2} - \beta^2 I_m(x) + \omega^2 L_1 C_1 I_m(x)\right] \cos(\omega t - \beta x) + \left[2\beta \frac{\partial I_m(x)}{\partial x} + \omega C_1 R_1 I_m(x) \cdot \left(1 + \frac{3}{4} \cdot \frac{I_m^2(x)}{I_0^2}\right)\right] \sin(\omega t - \beta x) = 0. \quad (6)$$

This is the first approximation of a nonlinear equation based on the method of harmonic balance. Equation (6) is followed by the equation for the current amplitude as a function of coordinate:

$$\frac{\partial I_m(x)}{\partial x} + \alpha I_m(x) \cdot \left(1 + \frac{3}{4} \cdot \frac{I_m^2(x)}{I_0^2}\right) = 0 \quad (7)$$

where $\alpha = \frac{R_1}{2Z_0}$ and $Z_0 = \sqrt{\frac{L_1}{C_1}}$ are the attenuation constant and the wave impedance of the line. The expression for the phase velocity ($v_{ph} = \beta/\omega$) can be derived from (6) and (7):

$$\beta^2 = \omega^2 L_1 C_1 + \frac{1}{I_m(x)} \cdot \frac{\partial^2 I_m(x)}{\partial x^2}. \quad (8)$$

Doing the integration of (7) with the boundary condition $I_m(x)\|_{x=0} = I_m(0)$ one obtains the current amplitude distribution along the line

$$I_m^2(x) = I_m^2(0) \cdot \frac{\exp(-2\alpha x)}{1 + \frac{3}{4} \cdot \frac{I_m^2(0)}{I_0^2} \cdot [1 - \exp(-2\alpha x)]}. \quad (9)$$

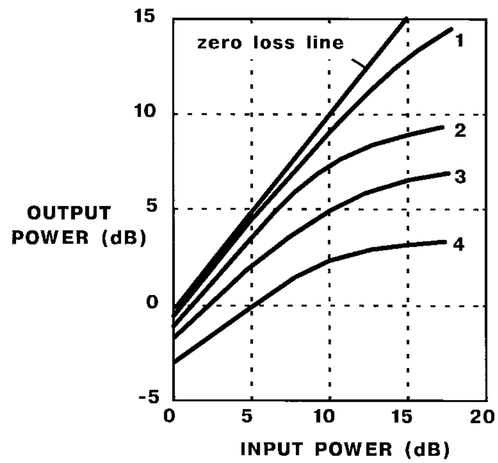

Fig. 1. Output power P_{out} as a function of input power P_{in} for the nonlinear transmission line section with different transmission coefficient α. P_{out} and P_{in} are normalized to the characteristic power P_o α (dB): 1—(-0.1); 2—(-0.5); 3—(-1.0); 4—(-2.0).

For the line section of the length l the relation between the input power P_{in} and output power P_{out} takes the form:

$$P_{\text{out}} = P_{\text{in}} \cdot \frac{\exp(-2\alpha l)}{1 + \frac{3}{4} \cdot \frac{P_{\text{in}}}{P_0} \cdot [1 - \exp(-2\alpha l)]} \quad (10)$$

where $P_0 = \frac{1}{2} \cdot I_0^2 \cdot Z_0$ is the characteristic power of the nonlinear transmission line.

C. Comparison with Experiment

Fig. 1 shows the dependence of the output power on the incident power normalized to P_0 for the nonlinear transmission line section. A set of curves corresponds to different initial values of the section transmission coefficient $a = -8.68 \log \alpha l$. It is easy to see from Fig. 1 that an essential rate of limitation of the signal can be obtained, if the initial loss of the line is high enough. If it is necessary to design a signal limiter with low-loss level with respect to the small signal, the effect of the power limitation could be enhanced by using resonant circuits containing the nonlinear superconducting films [9], [10]. Fig. 2 shows the comparison between the experimental results [12] and the data simulated using the expression (10). The experiment was performed with a coplanar line section of 7 mm length made from polycrystalline YBCO film with $T_c =$ 80 K. The model parameters are given in the legend to Fig. 2. The small signal surface resistance of the film was chosen in the model to provide the simulated small signal attenuation identical to that in the experiment. The rather good agreement of the simulated and experimental data provides support for the acceptability of the phenomenological description specified by (2).

III. Nonlinear Microstrip Resonator

A. Linear Characteristics of the Resonator

Fig. 3 shows the diagram of the microstrip resonator considered. The length of the resonator microstrip line section is $2l$. The resonator is coupled with the external circuits by

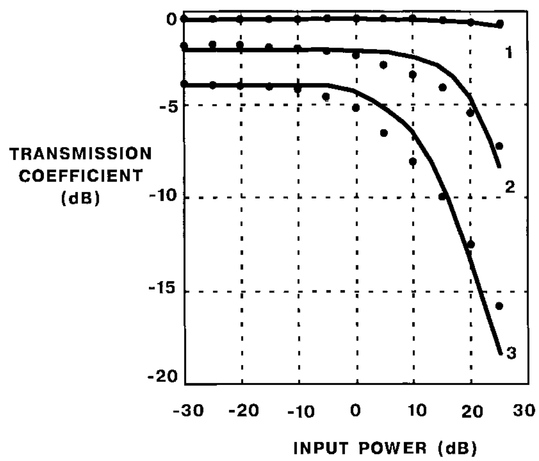

Fig. 2. Experimental and simulated transmission coefficient as a function of input microwave power $P_{\rm in}/P_{\rm o}$ for YBCO coplanar line section at different temperatures. Solid lines correspond to simulated data; dots correspond to experimental results from [12]. In the figure, T/T_c: 1: 0.05; 2: 0.7; 3: 0.9; model parameter $P_{\rm o}$: 1—100 mW; 2: 30 mW; 3: 6 mW.

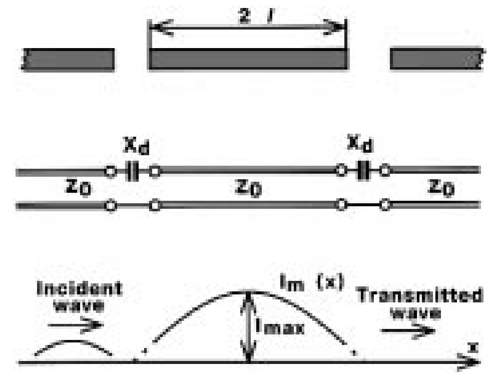

Fig. 3. Diagram of microstrip resonator and current amplitude distribution along the resonator with respect to the first harmonic of the signal.

capacitive gaps.[1] The transmission coefficient of the resonator at the resonant frequency is given by

$$\|S_{21}(\omega_0)\|^2 = \left(1 + \frac{Q_E}{Q_U}\right)^{-2} \tag{11}$$

where Q_U is the unloaded quality factor

$$Q_U = \frac{\pi \cdot Z_s}{R_1 \cdot 2l} \tag{12}$$

Q_E is the external quality factor

$$Q_E = \frac{\pi \cdot X_c^2}{4Z_0 Z_s} \tag{13}$$

Z_s is the wave impedance of the resonator microstrip line, and X_c is the reactance of the capacitive gaps. The relation between the resonator length $2l$ and the wave length λ in the transmission line for the first harmonic of oscillation is given by the following expression:

$$l = \frac{\lambda}{4} \cdot \left(1 + \frac{\Delta l}{l}\right); \qquad \frac{\Delta l}{l} = -\frac{2}{\pi} \cdot \frac{Z_s}{X_c} \tag{14}$$

where Δl is shortening the resonator line section in accordance with the resonance condition in the case of the capacitive coupling.

B. Maximum Microwave Current Amplitude in the Resonator

In order to start an estimation of nonlinear effects in the resonator, the amplitude of the microwave current in the resonator should be found. We shall denote through $I_{\max}$ the maximum of the standing wave amplitude in the resonator at the resonant frequency. The higher the quality factor of the resonator, the higher the current amplitude in the resonator. That is why in the case of the high quality factor of the resonator, the nonlinear effects are revealed under a low level of the incident microwave power. The distribution of the current amplitude along the resonator microstrip section is determined as

$$I_m(x) = I_{\max} \cos\left(\frac{2\pi}{\lambda} x\right). \tag{15}$$

The current amplitude at the ends of the resonator microstrip section can be found from the current distribution (15), being written in the form:

$$I_m(l) = I_m \cos\left[\frac{2\pi}{\lambda} \cdot \frac{\lambda}{4} \cdot \left(1 - \frac{2}{\pi} \cdot \frac{Z_s}{X_c}\right)\right] \tag{16}$$

where the resonator shortening is taken into account. For $Z_s \ll X_c$ one has

$$I_m(l) \cong I_{\max} \cdot \frac{Z_s}{X_c}. \tag{17}$$

The current determined by (17) is equal to the current amplitude of the traveling wave in the line connected to the output end of the resonator. In the input line the current is determined by the interference of incident and reflected waves. In order to specify the current amplitude for the wave which is incident upon the input port of the resonator, the following relation should be used:

$$I_{\rm incid} = I_m(l) \cdot \frac{1}{\|S_{21}(\omega_0)\|}. \tag{18}$$

Thus, combining (11), (17), and (18), one obtains the ratio of the maximum resonator standing wave amplitude to the amplitude of the incident wave

$$\frac{\|I_{\max}\|}{\|I_{\rm incid}\|} = \sqrt{\frac{4}{\pi} \cdot \frac{Z_0}{Z_s} \cdot Q_E}\left(1 + \frac{Q_E}{Q_U}\right)^{-1}. \tag{19}$$

The maximum current amplitude $I_{\max}$ as a function of the rate of coupling the resonator Q_E/Q_U with the external circuits for the case of $Z_S = Z_0$ is illustrated in Fig. 4.

C. The Nonlinearity of the Microstrip Resonator with Respect to the First Harmonic of the Signal

In accordance with the suggested phenomenological description (2) of the resistance of the line as a function of the instantaneous value of the current, and taking into account

[1] Commonly the capacitive gap is presented by an equivalent π-circuit. We use a simplified presentation by a series capacitance only.

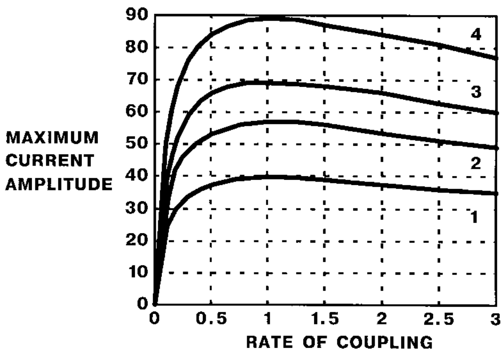

Fig. 4. Maximum current amplitude at the center of the microstrip resonator as a function of the rate of coupling Q_e/Q_u for different unloaded quality factor Q_u: 1—5000; 2—10 000; 3—15 000; 4—25 000. Maximum current amplitude is normalized to the incident wave current amplitude.

(5) and (15), the resistance per unit length of the resonator microstrip section should be defined as

$$R_1(x,t) = R_1 \cdot \left[1 + \frac{I_{\max}^2}{I_0^2} \cdot \cos^2\left(\frac{2\pi x}{\lambda}\right) \cdot \cos^2 \omega t\right]. \quad (20)$$

The power of the microwave signal which is dissipated in the resonator can be calculated upon integrating with respect to coordinate along the resonator microstrip line section and with respect to time over the period of microwave oscillations

$$P_{\text{diss}} = \frac{1}{2\pi} \cdot \int_{-\pi}^{\pi} \int_{-l}^{l} I_{\max}^2 \cdot \cos^2(\frac{2\pi x}{\lambda}) \cdot \cos^2(\omega t) \cdot R_1(x,t) dx d(\omega t). \quad (21)$$

The integration results in

$$P_{\text{diss}} = \frac{1}{2} \cdot I_{\max}^2 \cdot R_{\text{eff}} \quad (22)$$

where

$$R_{\text{eff}} = R_1 \cdot l \cdot \left(1 + \frac{9}{16} \cdot \frac{I_{\max}^2}{I_0^2}\right). \quad (23)$$

In line with the result obtained, the effective unloaded quality factor should be introduced

$$Q_{U,\text{eff}} = Q_U \cdot \left(1 + \frac{9}{16} \cdot \frac{I_{\max}^2}{I_0^2}\right)^{-1}. \quad (24)$$

Now we use the expression for the maximum current in the resonator (19), in which Q_U should be replaced by $Q_{U,\text{eff}}$. After replacing Q_U by $Q_{U,\text{eff}}$ in (19) and substituting (19) into (24) one obtains

$$\frac{Q_U}{Q_{U,\text{eff}}} = 1 + \frac{9}{4\pi} \cdot \frac{I_{\text{incid}}^2}{I_0^2} \cdot \frac{Z_0}{Z_s} \cdot Q_E \left(1 + \frac{Q_E}{Q_{U,\text{eff}}}\right)^{-2}. \quad (25)$$

The formula obtained is the equation with respect to $Q_{U,\text{eff}}$, which can be found as a function of I_{incid} for fixed values of Q_U and Q_E. In line with (11), the transmission coefficient of the resonator is

$$\|S_{21}\|^2 = \left(1 + \frac{Q_E}{Q_{U,\text{eff}}}\right)^{-2} \quad (26)$$

where $Q_{U,\text{eff}}$ is determined as a solution to (25). Therefore, the transmission coefficient can be found as a function of I_{incid} or P_{incid}.

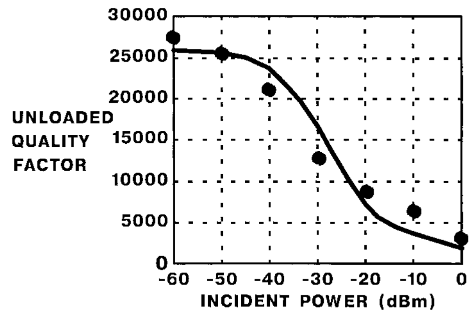

Fig. 5. Effective unloaded microstrip resonator quality factor versus the incident power simulated in accordance with (25). Dots are the experimental data from [12].

D. Comparison with Experiment

Fig. 5 shows the simulated effective unloaded quality factor of the resonator $Q_{U,\text{eff}}$ as a function of the incident power. In Fig. 5 the experimental data [13] are shown as well. In order to fit the simulated data to the experimental ones, the following fitting parameters were used: $P_0 = 5$ mW, $Q_E = 26\,000$. The equal values of unloaded and external Q-factors were assumed: $Q_U = Q_E$. One can see a good agreement between experimental and simulated data. Attention should be drawn to the fitting parameter P_0 which was found to be in the same order of magnitude in both resonator and traveling wave experiments.

IV. Generation of Third Harmonic of Signal Due to Nonlinearity of Microstrip Resonator

A. Amplitude of the Third Harmonic Current in the Microstrip Resonator

The inertialessness of the superconducting film nonlinearity provides for HTS film up to 100 GHz the simultaneous response of the film to the microwave current. The product of the first harmonic current and the nonlinear term in the resistance per unit length sets up the third harmonic electric field along the microstrip line section of the resonator

$$E_3(x,t) = \frac{1}{4} \cdot I_{\max} R_1 \cdot \frac{I_{\max}^2}{I_0^2} \cdot \cos^3\left(\frac{2\pi x}{\lambda}\right) \cdot \cos(3\omega t). \quad (27)$$

The third harmonic current along the resonator section can be written in the form:

$$I_3(x,t) = I_{\max,3} \cdot \cos\left(\frac{6\pi x}{\lambda}\right) \cdot \cos(3\omega t) \quad (28)$$

where $I_{\max,3}$ is the maximum of the third harmonic current amplitude in the resonator. Now we can calculate the third harmonic power generated in the resonator due to the nonlinearity of the superconducting film:

$$P_3 = \frac{1}{2\pi} \cdot \int_{-\pi}^{\pi} \int_{-l}^{l} \cdot E_3(x,t) \cdot I_3(x,t) dx d(\omega t). \quad (29)$$

Substituting (27) and (28) into (29) and doing integration, one obtains

$$P_3 = \frac{1}{32} \cdot I_{\max} \cdot I_{\max,3} \cdot \frac{I_{\max}^2}{I_0^2} \cdot R_1 l. \quad (30)$$

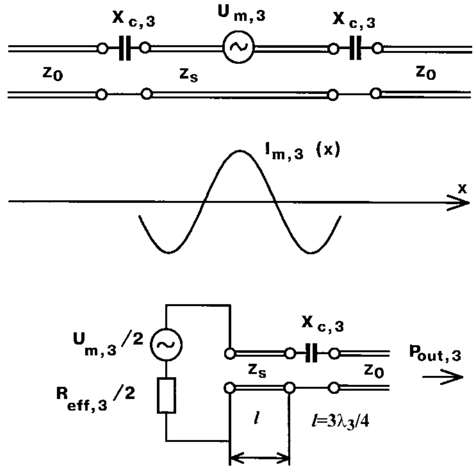

Fig. 6. Diagram of microstrip resonator and current amplitude distribution along the resonator with respect to the third harmonic of the signal.

According to the equivalent circuit (Fig. 6), the load impedance Z_{load} referred to the maximum of the third harmonic current is

$$Z_{\mathrm{load},3} = \frac{2Z_s^2}{Z_0 - i\frac{1}{3}X_c} - iX_{c,0} + R_{\mathrm{eff},3} \tag{31}$$

where $R_{\mathrm{eff},3}$ is responsible for an intrinsic linear loss of the resonator at the third harmonic frequency, $X_{c,0}$ is an additional parasitic reactance in the circuit. Let us assume that the resonator is in the state of resonance with respect to the third harmonic as well as to the first one. Hence, the imaginary part of the load impedance should be canceled. Then, taking into account that $X_c \gg Z_0$ and that $R_{\mathrm{eff},3} = 9R_{\mathrm{eff},1}$, and using expressions (12), (13), and (24), one obtains $R_{\mathrm{load},3}$ as a real part of (31)

$$R_{\mathrm{load},3} = 18 \cdot \frac{\pi Z_s}{4}\left(\frac{1}{Q_E} + \frac{1}{Q_{U,\mathrm{eff}}}\right). \tag{32}$$

Thus

$$P_3 = \frac{1}{2}I_{\max,3}^2 R_{\mathrm{load},3} = \frac{9\pi}{4} \cdot I_{\max,3}^2 Z_s\left(\frac{1}{Q_E} + \frac{1}{Q_{U,\mathrm{eff}}}\right). \tag{33}$$

Equating (30) and (33) results in

$$I_{\max,3} = \frac{1}{144} \cdot \frac{I_{\max}^3}{I_0^2} \cdot \frac{1}{Q_U}\left(\frac{1}{Q_E} + \frac{1}{Q_{U,\mathrm{eff}}}\right)^{-1}. \tag{34}$$

B. Third Harmonic Power in the Resonator

Now we can calculate the third harmonic power $P_{\mathrm{out},3} = 0.5 \cdot I_{m,3}^2(l)Z_0$ emitted in one port of the resonator, where $I_{m,3}(l)$ can be found using (34) and (17). Thus, taking into account (13) one obtains

$$P_{\mathrm{out},3} = \frac{1}{2} \cdot \left(\frac{1}{144}\right)^2 \cdot \frac{I_{\max}^6}{I_0^4} \cdot \frac{1}{Q_U^2} \cdot \left(\frac{1}{Q_{U,\mathrm{eff}}} + \frac{1}{Q_E}\right)^{-2} \cdot \frac{9\pi Z_s}{4Q_E}. \tag{35}$$

According to (19), the current amplitude at the center of the resonator $I_{\max}$ can be expressed through the current amplitude of the incident wave and consequently through the incident power: $(I_{\mathrm{incid}}/I_0)^2 = P_{\mathrm{incid}}/P_0$. Thus, we have

$$P_{\mathrm{out},3} = \frac{1}{(12\pi)^2} \cdot \frac{P_{\mathrm{incid}}^3 Q_E^2}{P_0^2} \cdot \frac{\left(\frac{Q_E}{Q_U}\right)^2}{\left(1 + \frac{Q_E}{Q_{U,\mathrm{eff}}}\right)^8}. \tag{36}$$

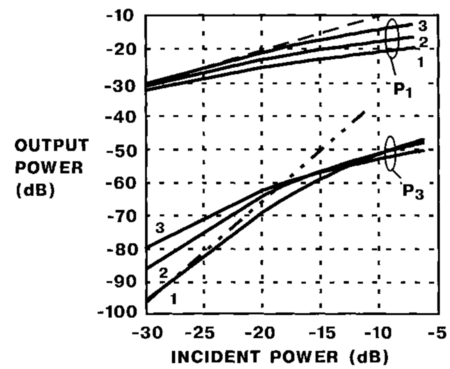

(a)

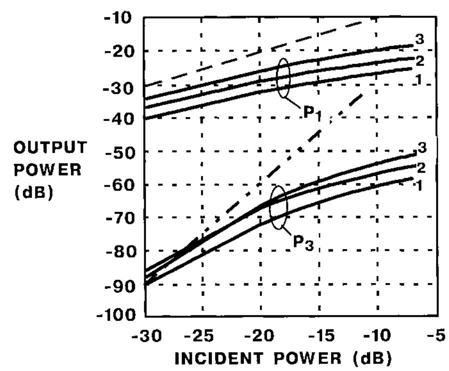

(b)

Fig. 7. Output power of first (P_1) and third (P_3) harmonics as functions of incident power P_{incid}. The power is normalized to the characteristic power P_0. (a) Q_u=10 000; Q_e: 1: 500, 2: 1000, 3: 2000; (b) Q_u=1000; Q_e: 1: 500, 2: 1000, 3: 2000. In the figure, dashed line corresponds to the slope of power 1; dashed-dotted line corresponds to the slope of power 3.

C. Some Numerical Results for the First and the Third Harmonics as Functions of the Incident Power

Thus, we have relations (26) and (36) for the output power of the first and the third harmonics as functions of the incident power. The result obtained is correct for the case $P_{\mathrm{out},3} \ll P_{\mathrm{out},1}$ because the back transformation of the third harmonic into the first one is not taken into account. Fig. 7 illustrates relations (26) and (36). It should be noticed that for a weak coupling of the resonator with external circuits [Fig. 7(a)] and a low level of the incident power, the slope of the curves for the first and the third harmonics correspond to the power 1 and 3 with respect to the incident microwave power. However, the stronger the coupling [Fig. 7(b)] and the higher the level of the incident microwave power, the smaller the slopes of the output power curves of the first and the third harmonics. The change of the slope of the third harmonic output power curves was observed experimentally [14], [15] and can be explained by the change of the quality factors of the resonator under the influence of the incident power.

V. Conclusion

The simplest model of the superconducting microstrip line nonlinearity has been used for a description of nonlinear phenomena in a microstrip transmission line and a microstrip resonator. The theoretical results are adequate to the experiments not only qualitatively, but quantitatively with good accuracy. Only one fitting parameter of the model is used. It is the characteristic power of the microstrip line P_0. For a few experimentally studied lines the characteristic power of the microstrip line P_0 is approximately a few milliwatts. For the transmission line with $Z_0 = 50\ \Omega$, it corresponds to the characteristic current about 0.01 A, that is smaller than the critical current of the strip with respect to the direct current. Remaining on the phenomenological level of the method of attack, we have to say that the numerical data for the nonlinearity of the microstrip lines should be collected and used to set up the correlation between the characteristic power of the microstrip line and the characteristics of the film processing: stoichiometry, structure, and the peculiarities of the film pattern process. The correlation found will make it possible to develop recommendations for improvement of the high power handling of the superconducting microstrip components.

References

[1] J. Halbritter, "Change of eigenstate in a superconducting RF cavity due to a nonlinear response," *J. Appl. Phys.,* vol. 41, no. 11, pp. 4581–4588, Nov. 1970.

[2] W. H. Hartwig, "Superconducting resonator and devices," *Proc. IEEE,* vol. 61, no. 1, pp. 58–69, Jan. 1973.

[3] M. M. Gaidukov, O. G. Vendik, and S. G. Kolesov, "Microwave power limiter based on high Tc superconducting film," *Electron. Lett.* vol. 26, no. 16, pp. 1229–1230, Aug. 1990.

[4] S. T. Ruggiero, A. Cardonna, and H. R. Fetterman, "Mixing in Tl-CaBaCuO superconducting films at 61 GHz," *IEEE Trans. Magn.,* vol. 27, no. 2, pp. 3070–3072, Feb. 1991.

[5] A. M. Portis *et al.,* "Power and magnetic field induced microwave absorption in Tl-based high Tc superconducting films," *Appl. Phys. Lett.,* vol. 58, no. 3, pp. 307–309, Jan. 1991.

[6] J. Halbritter, "On extrinsic effects in the surface impedance of cuprate superconductors by weak links," *J. Appl. Phys.,* vol. 71, no. 1, pp. 339–343, Jan. 1992.

[7] D. E. Oates *et al.,* "Modeling of linear and nonlinear effects in striplines," *J. Superconducting,* vol. 5, no. 4, pp. 361–369, Apr. 1992.

[8] C. C. Chiu, D. E. Oates, G. Dresselhaus, and M. S. Dresselhaus, "Nonlinear electrodynamics of superconducting Nb and NbN thin films at microwave frequencies," *Phys. Rev. B,* vol. 45, no. 9, pp. 4788–4798, Sept. 1992.

[9] A. B. Kozyrev, T. B. Samoilova, and S. Yu. Shaferova, "Nonlinear surface resistance and frequency mixing in superconducting films," *Superconducting Sci. Technol.,* vol. 7, no. 10, pp. 777–782, Oct. 1994.

[10] V. N. Keis, A. B. Kozyrev, T. B. Samoilova, and O. G. Vendik, "High speed microwave filter-limiter based high T_c superconducting films," *Electron. Lett.* vol. 29, no. 6, pp. 546–547, Mar. 1993.

[11] T. B. Samoilova, "Nonlinear microwave effects in thin superconducting films," *Superconducting Sci. Technol.,* vol. 8, no. 5, pp. 259–276, 1995.

[12] O. G. Vendik *et al.,* "Microwave power effect on transmission characteristics of the transmission line based on YBa2Cu3O7-x film," *Superconductivity, Physics, Chemistry, Technol.,* vol. 3, no. 6, pp. 1040–1043, Jun. 1990.

[13] G. L. Hey-Shipton, "Power rating of multi-resonator HTS filters," in *IEEE MTT-S Workshop Notes: High Power Superconducting Microwave Technology,* San Diego, CA, May 1994.

[14] D. E. Oates and A. C. Anderson, "Surface impedance measurements of YBa2Cu3O7-x thin films in stripline resonators," *IEEE Trans. Magn.,* vol. 27, no. 2, pp. 867–871, Feb. 1991.

[15] A. M. Ferendeci *et al.,* "Two-tone intermodulation distortion in high-Tc superconducting thin films," *Proc. SPIE,* vol. 2156, pp. 116–122, 1994.

Orest G. Vendik (M'94) was born in Leningrad, USSR, in 1932. He received the Diploma of Radio Engineering, Candidate of Sc. Degree (Ph.D.), and Doctor of Sc. degree in 1954, 1957, and 1966, respectively, from Leningrad Electrical Engineering Institute (now St. Petersburg Electrotechnical University), St. Petersburg, Russia.

In 1964 he joined St. Petersburg Electrotechnical University as a Professor in the Department of Applied Physics. From 1969–1989 he held the position of Head of the Department of Electron–Ion Technology. He is currently Professor of the same department, as well as Head of the Cryoelectronics Group. His research interests have been in foundation of solid state electronics (ferrites, ferroelectrics, superconductors) and microwave physics. His concentration is on properties and applications of HTSC's and ferroelectrics at microwaves. He takes part in elaboration of microwave components based on S–N (superconducting–normal) transition and voltage controlled ferroelectrics: signal limiters, switches, and phase shifters.

Dr. Vendik is a member of the St. Petersburg Association of Scientists.

Irina B. Vendik (M'96) received the Electronics Engineer Diploma and Candidate of Sc. (Ph.D.) from Leningrad Electrical Engineering Institute (now St. Petersburg Electrotechnical University), St. Petersburg, Russia, in 1959 and 1964, respectively, and the Doctor of Sc. (Physics) Degree from A. F. Ioffe Physicotechnical Institute, St. Petersburg, in 1990.

She is Professor of the Department of Microelectronics and the Head of the Microwave CAD Group at St. Petersburg Electrotechnical University. Her general research interests have been in foundations of solid-state physics and microwave electronics: low-dimensional crystals at microwaves, p–i–n diode switches and phase shifters, and microwave applications of high-T_c superconductors (HTS). Her current activity is in the area of elaboration of HTS microwave components: filters, dividers, switches, and phase shifters. She is also interested in a development of CAD-oriented models of HTS planar components.

Tatyana B. Samoilova received the Electronics Engineer diploma in 1970, and the Candidate of Science Degree (Ph.D.) in physics and mathematics in 1986, from Leningrad Electrical Engineering Institute (now St. Petersburg Electrotechnical University), St. Petersburg, Russia.

She is an Associate Professor in the Electronics Department of St. Petersburg Electrotechnical University. Her general research interests have been in the investigations of physical properties of superconductors. Her current activity concentrates on the applications of high temperature superconductor films in microwave microelectronics.